# Optical Imaging for Diagnosis of Rheumatoid Arthritis
## *Automatic Versus Human Evaluation*

Pouyan Mohajerani[1], Reinhard Meier[2], Ernst J. Rummeny[2] and Vasilis Ntziachristos[1]
[1]*Institute for Biological and Medical Imaging, Technische Universität München and Helmholtz Zentrum München, Ingolstädter Landstrasse 1, Neuherberg 85764, Germany*
[2]*Department of Radiology, Klinikum Rechts der Isar, Technische Universität München, München, Germany*

Keywords: Optical Imaging, Fluorescence, Rheumatoid Arthritis (RA), Inflammation, Indocynine Green (ICG), Planar Illumination, Near-Infrared Dyes, Spatiotemporal Analysis, Principal Component Analysis (PCA).

Abstract: Successful detection of rheumatoid arthritis (RA) at the early stages of development can significantly enhance the chances of effective therapy. The early onset of RA is often marked with inflammation of the synovial lining of the joint, a condition known as synovitis. Effective imaging of synovitis is therefore of critical importance. While dynamic, contrast-enhanced magnetic resonance imaging (MRI) is capable of effective imaging of synovitis, it is a costly modality. As an alternative, inexpensive approach, optical imaging post injection of the near-infrared fluorescent dye indocynine green (ICG) has been recently proposed for imaging RA. Evaluation of the obtained optical images is performed via examination by trained human readers. However, optical imaging has yet to achieve the diagnostic accuracy of MRI. In this paper we present a method for automatic evaluation of the fluorescence images and compare its performance with the human-based evaluation. Our method relies on our previous work on spatiotemporal analysis of image sequence with principal component analysis (PCA) to seek synovitis signal components with the help of a segmentation method. The results for a group of 600 joints, obtained from 20 patients, suggest improved diagnostic performance using the automatic approach in comparison to human-based evaluation.

## 1 INTRODUCTION

Imaging can play a critical role in developing effectively and timely therapeutic approaches for treating rheumatoid arthritis (RA) by the way of early detection of synovitis (Emery and Quinn, 2003, Ostergaard et al., 2005). Synovitis is the condition of the inflammation of the synovial lining surrounding the joint and marks the onset of RA. Conventionally, X-ray computed tomography (CT) has been employed to image bone and joint damage resulting from joint inflammation (Backhaus et al., 1999). In this sense CT is often applicable in the later stages of RA development. Other anatomical modalities, particularly magnetic resonance imaging (MRI) in conjunction with MR contrast agents and ultrasound have been employed for early detection of RA (Emery et al., 2007). Nevertheless, such methods are often limited by factors such as operator dependency for ultrasound (Delle Sedie et al., 2008) and high costs for the MRI, (Emery et al., 2007)).

As an alternative, cost-effective approach, optical imaging (OI) has been proposed for imaging RA (Chen et al., 2005, Hielscher et al., 2004, Fischer et al., 2010, Mohajerani et al., 2013, Mohajerani et al., 2014, Meier et al., 2012, Gompels et al., 2010). Several planar and tomographic approaches have been proposed, relying on the physiological changes in joint tissue as a source of optical contrast (Hielscher et al., 2011, Klose et al., 1999).

The application of fluorescence has been also recently proposed for imaging RA in both planar (Meier et al., 2012, Werner et al., 2012) and tomographic (Mohajerani et al., 2014) modes. These approaches use the organic, near-infrared fluorescence dye indocynine green (ICG) to create optical contrast in affected tissue. Specifically, the intravenously injected ICG tends to accumulate in inflamed synovial tissue, a feature which enables differentiation of the inflamed joints from healthy joints using measured fluorescence signals. In particular, planar imaging operating in epi-illumination mode offers the ability to image all hand joints in both hands simultaneously (Meier et al., 2012, Meier et al., 2014, Werner et al., 2012).


Mohajerani P., Meier R., Rummeny E. and Ntziachristos V..
Optical Imaging for Diagnosis of Rheumatoid Arthritis - Automatic Versus Human Evaluation.
DOI: 10.5220/0005217200360043
In *Proceedings of the International Conference on Bioimaging* (BIOIMAGING-2015), pages 36-43
ISBN: 978-989-758-072-7

The acquired fluorescence images are examined by a trained human reader, who assigns semi-quantitative inflammation scores to different joints upon examining the entire acquired image sequence. An example an acquired fluorescence image in comparison to the corresponding MRI scan is presented in Figure 1.

Planar, ICG-enhanced imaging of RA is a promising approach which has been applied for both diagnostic (Thomas Dziekan et al., 2011, Meier et al., 2012) as well as therapy monitoring purposes (Meier et al., 2014). While offering a cost-effective and rapid imaging alternative, the diagnostic accuracy of the method is compromised, in particular in comparison with contrast-enhanced MRI, which serves as the gold standard in evaluation studies (Meier et al., 2012).

One reason for the relatively (compared to MRI) low diagnostic accuracy of OI, is the presence of strong signal interference (Meier et al., 2012). Specifically, the fluorescence signal emanating from the underlying synovitis is strongly coupled to other signals originating from the dorsal veins as well as other tissues. This interference occurs in both spatial and temporal dimensions and complicates the inference process as performed by a human reader. We have previously reported a spatiotemporal analysis approach for decoupling the signal components in the acquired image sequence using principal component analysis (PCA) (Mohajerani et al., 2013).

In this paper, we present automatic detection of the synovitis, as an alternative to the human-based detection. We further evaluate and compare the automatic detection method with the human-based detection for a cohort consisting of 20 patients.

## 2 IMAGING METHODOLOGY

Fluorescence imaging was performed with a planar, near-infrared fluorescence imaging system (Xiralite X4, Mivenion GmbH, Berlin, Germany. This system enables real-time image acquisition at the fluorescence wavelength of ICG (around 830 nm) simultaneously from both of the hands after epi-illumination excitation applied to the dorsal hand sides. The patients received a bolus injection pf ICG at a dosage of 0.1 mg per kg body weight. A total of 360 images were obtained at the fluorescence wavelength of ICG, with a frame rate of 1 fps.

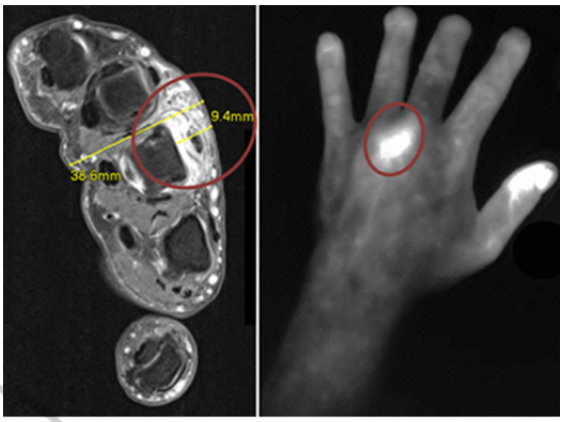


Figure 1: Optical imaging of rheumatoid arthritis shown in the left panel for the left hand of a 42 year old male patient. This patient exhibited severe arthritis in the 3rd metacarpophalangeal (MCP) joint. The right panel depicts the corresponding transversal slice of the T1-weighted fat-saturated contrast-enhanced MRI image in the MCP region. The higher accumulation of the contrast agents in the MCP 3 joint have resulted in higher signal intensities in both MRI and optical images.

## 3 SPATIOTEMPORAL ANALYSIS

Non-specific fluorescence signal interfering with the target fluorescence emanating from synovitis complicated the diagnosis. The interference takes place both in the intra-frame domain (spatial interference) as well as in the inter-frame domain (temporal interference). Decoupling such signal components in both spatial and temporal domains might therefore help with more accurate diagnosis.

We have recently presented spatiotemporal analysis for decomposing the signal components in the fluorescence image sequences (Mohajerani et al., 2013). This method makes use of the principal component analysis (PCA) (Jolliffe, 2002), as an orthogonal de-correlating transformation, to covert the original sequence into a group of sequences, each bearing distinct spatiotemporal components. Herein we briefly review this approach.

Specifically, consider a set of fluorescence images $I_p$ for $p = 1 \ldots P$, where each image has a size of $M_1 \times M_2$ pixel size ($P$ was equal to 360). Prior to the PCA analysis, two levels of localization were performed on the raw image sequence $I_p$. The first step limits the processing to a specific region within each image, achieved via a region of interest defined accordingly for each of the joints, as shown in Figure 2. The second localization step confines he PCA processing to windowed subsequence of the

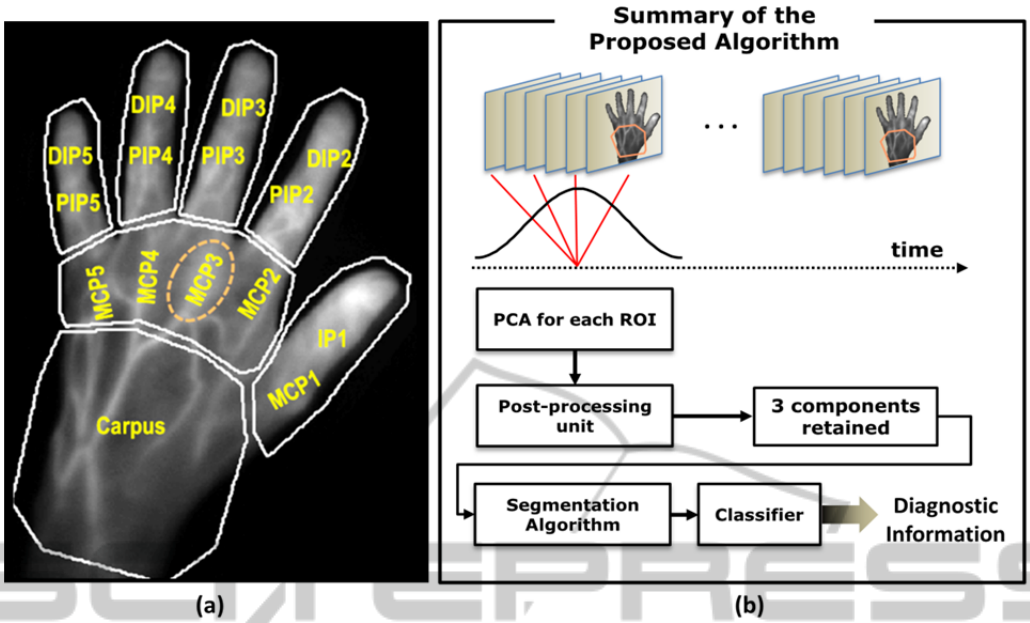


Figure 2: The proposed methodology of automatic detection of rheumatoid arthritis (a) partitioning the fluorescence image into 7 regions for the carpus, MCP region and each of the fingers. (b) PCA-based processing and segmentation-based detection within each ROI (here, the carpus ROI). The results of the PCA processing are to then fed to the segmentation approach. The metric values assigned by the segmentation method to different signal components are then classified to achieve diagnostic information regarding each joint.

images within each ROI. These two localization steps were performed to improve the performance of PCA in decoupling image components, as the signal dynamics change significantly across time and space. For each of the 7 ROIs shown, a 2-D subsequence of images $J_p$ is defined from the original sequence. Next, $K$ successive images were taken from the subsequence $J_p$. This subsequence is defined as $H_i$, $i = 1$ to $K$. The PCA was then applied to this image sequence by first vectorising and stacking the images $H_i$, to achieve a $K \times M_1M_2$ matrix $\mathbf{X}$. Next, singular value decomposition (SVD) of the covariance matrix of $\mathbf{X}$ was obtained. and the resulting unitary matrix of its eigenvectors was applied as the PCA transformation matrix. The 3 components with the largest singular values were then retained and the rest of modes were discarded. These 3 retained components were then mapped to the blue, red and green channels of an output color sequence, according to their descending singular values. Further details of the PCA processing can be found in (Mohajerani et al., 2013). A summary of the steps involved can be further seen in figure 2.

The results of the spatiotemporal analysis for a specific joint of patient suffering severe inflammation in the 3rd MCP joint are presented in figure 3. As observed, the PCA-based method has successfully separated the synovitis signal from the background and vein signals into distinct PCA channels.

## 4 AUTOMATIC DETECTION OF RHEUMATOID ARTHRITIS

As previously noted, the synovitis signal is often coupled in time and space to interfering signals emanating from background tissue or dorsal veins. However, the synovitis signal is likely to appear as a distinct component in one of the PCA channels.

Here, we propose automatic detection of synovitis by searching through the PCA channels for a signal component attributable to synovitis. To this end, we use a segmentation approach previously proposed in (Mohajerani et al., 2013).

Specifically, for a specific joint, first an elliptical ROI is defined surrounding this joint. This ROI is denoted by the binary image $R$. The segmentation approach then applies a threshold to each PCA image. The thresholding results in a binary image $J$. Within the image $J$, the connected component with the largest overlap with $R$ is found and denoted by $K$. A metric is defined then to quantify the likelihood of the signal in the region $K$ to be due to synovitis. Specifically, $S(K,R)$ is defined as

$$S(K,R) = 3\times \left(1-\max\left(\frac{\max\left(d(K,R),r\right)}{r}, J(K,R), 1-E(K)\right)\right), \quad (1)$$

where $J(K, R)$ and $d(K, R)$ denote respectively the Jaccard (Michael Levandowsky and Winter, 1971) and Hausdorff (Huttenlocher et al., 1993) distances between $K$ and $R$ and $E(K)$ is the energy of the image $I$ within the label in $K$ (Mohajerani et al., 2013).

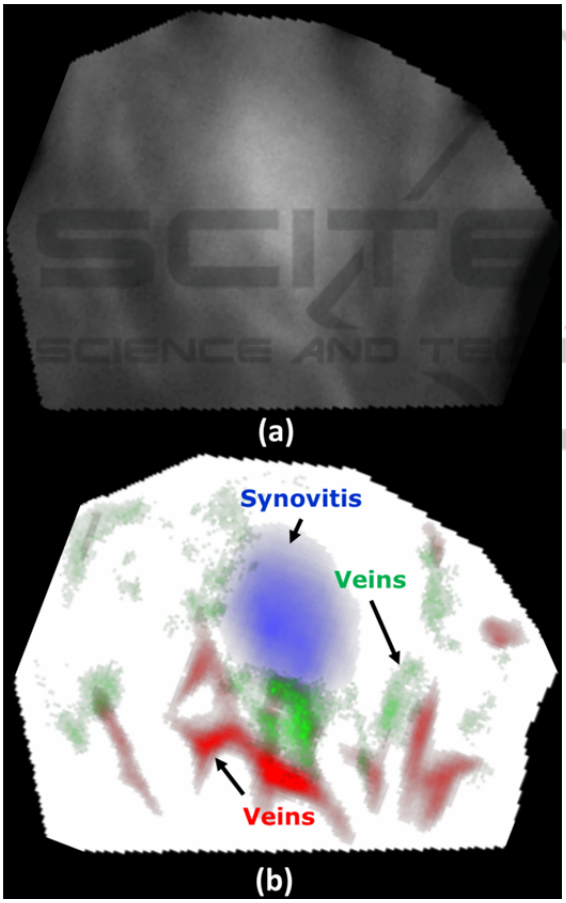


Figure 3: An example of the PCA-based spatiotemporal processing applied to the MCP-region of a patient with severe synovitis in the MCP 3 joint of the right hand. (a) Shows the measured raw fluorescence image, where the synovitis signal is coupled with background and dorsal vein signals. (b) The decomposed image obtained using the PCA-based approach, where the synovitis signal is mapped to the blue channel and is clearly distinct from the vein signals mapped to the green and red channels.

The metric $S(K,R)$ has a value between 0 and 3, where a higher value denotes a higher likelihood that the contours of $K$ delineate the synovitis signal in the corresponding PCA channel.

The automatic detection of the synovitis then operates as follows. All PCA images for all the blue, red and green channels are then processed with the segmentation method presented and the corresponding metric values are found. The component $K$ with the highest value of $S(K,R)$ across all channels in then designated as the synovitis signal. A summary of this approach is presented in figure 2. Figure 4 shows the results of the automatic detection method for a specific case of a patient with moderate synovitis in the left carpus. In this specific case, the component with the highest metric value appeared in the red channels, as shown by the black contour in figure 4(b).

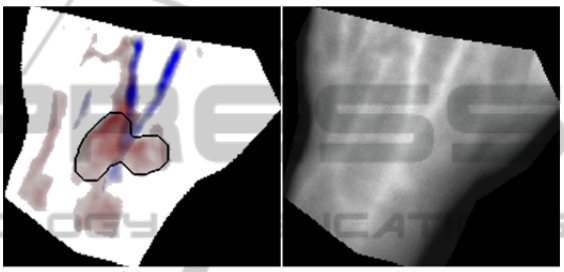


Figure 4: Case study of the automatic detection method proposed herein for the left carpus joint of a 49 year old female patient with moderate synovitis. (a) The blue and red PCA components for the carpus ROI, where the black contours denotes the detected synovitis signal in the red channel. The vein signal was mapped to the blue channel and there was no conspicuous signal in the green channel. (b) The corresponding raw fluorescence image. The scores assigned by the 4 human readers to this joint consisted of 0, 0, 0 and 1.

## 5 CLINICAL EXAMINATION AND COHORT INFORMATION

The development presented and performed in this paper have been conducted in the context of a recent study carried out at the Klinikum rechts der Isar, Munich, Germany, which aimed at of evaluating the diagnostic performance of ICG-aided imaging of RA (Meier et al., 2012).

The automatic detection method proposed herein was applied to fluorescence image sequences

Table 1: Distribution of inflammation severity among the 600 hand joints of the 20 patients recruited in this study.

| | Healthy | Mild | Moderate | Severe |
|---|---|---|---|---|
| Carpus | 16 | 16 | 5 | 3 |
| MCP | 93 | 90 | 16 | 1 |
| PIP/DIP | 326 | 28 | 5 | 1 |

obtained from a group of 20 patients (14 females, 6 males, aged 41±16). The patients were examined and imaged with contrast-enhanced MRI using a 3T MR machine (Verio, Siemens Erlangen, Germany) and a protocol described in (Meier et al., 2012). MR-based synovitis scores of 0 to 3 (healthy to severe) were assigned to each of the 600 joints.

Three radiologists scored the degree of inflammation in a total of 30 joints of both hands using the MR scans. Synovitis scores on a 4-point-ordinate scale (0: no inflammation, 1: mild, 2: moderate, 3: severe) were assigned to each joint according to the semi-quantitative assessment system suggested by the OMERACT MRI group (Ostergaard et al., 2003). The MR scores constitute the true diagnostic information, as explained in the next section.

Similarly, the fluorescence images were scores by the 3 radiologists, with a repeated 4$^{th}$ scoring performed after 4 weeks, as explained in (Meier et al., 2012). As such, 4 scores between 0 and 3, are obtained for each of the 30 hand joints for each patient. These scores are then used to evaluate human-based evaluation of the optical images, in comparison to the proposed, automatic method. The distributions of synovitis severity within different joint groups (interphalangeal, metacarpophalangeal and carpal) are shown in Table 1, according to the examination results of the MR scans.

## 6 EVALUATION METHODOLOGY

The localization metric devised in Section 4 yields a value between 0 and 100 (with 100 designating highly likelihood of being an inflammation signal) to each signal component. A threshold can be applied to this localization metric toward making a decision about synovitis severity of a given joint. The results can be demonstrated using the so-called receiver operating characteristic (ROC) curves, denoting as sensitivity vs specificity.

ROC curves denote the classification performance of a binary classifier (Zou et al., 2007). It should be noted that the $x = y$ on the ROC plane corresponds to random classification. Therefore, any curve above this line is desirable. The optimal performance corresponds to the upper-left corner (sensitivity = specificity = 100%). One way to compare different ROC curves is to compare the area under curve (AUC). The AUC is a measure of a classifier's quality (Fawcett, 2006). The optimal classifier has an AUC of 1.

To achieve a binary classifier, we consider two modes of classification. In classification 1, the threshold is applied to the segmentation metric to make a decision between healthy and affected (mild, moderate or severe synovitis) joints. In classification II, a decision was made between joints with "no or mild synovitis" and joints with "moderate or severe synovitis".

Three diagnosis methods are examined and evaluated in this work:

- Method A: Human evaluation of raw images
- Method B: Automatic evaluation of raw images
- Method C: Automatic evaluation of PCA images

Method A is the conventional method used currently in the clinic (Meier et al., 2012). Method C constitutes the proposed method. We have already shown using a cohort of 15 patients that the method C outperforms method B (Mohajerani et al., 2013).

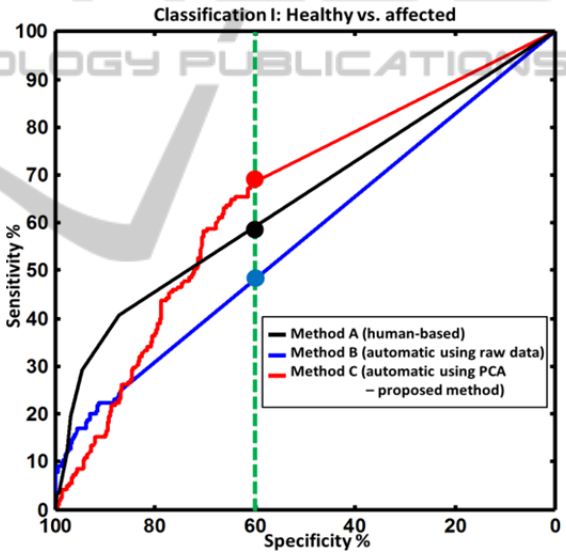


Figure 5: Receiver operator characteristic (ROC) curves for classification I: healthy joints versus affected joints (mild, moderate or severe synovitis). The ROC curves are shown using three methods: segmentation of the raw images (blue curve), segmentation of the PCA components (red curve, the proposed method) and the human-based evaluation (black curve). The green, dotted vertical line denotes a detection specificity of 60%. For this value, the proposed approach outperforms the human evaluation by achieving a sensitivity of more than 70% (human evaluation had a sensitivity of around 55%). For higher values of specificity (more than 70%), all methods showed poor sensitivity of less than 50%.

In this paper, we examine the performance of the proposed method (method C), in comparison with the human-based read (method A), for the first time.

The results are presented in the next section. For method A, the synovitis score was taken as the medium of the 4 scores obtained by the 4 readers (as explained in Section 2). For methods B and C, the synovitis score was the metric *S*, shown in Eq. 1.

## 7 DIAGNOSTIC PERFORMANCE RESUTLS

Figure 5 shows the ROC curves for classification I, as defined in the previous section. The proposed method (method C, red curve) showed slightly better performance than the other two methods for the specificity value of 60% (marked with filled circles). Over all, both automatic and human-based detection had an equal performance in terms of the AUC values, as shown in Table 2.

Table 2: Area under curve (AUC) values for the three detection methods for classification I (healthy vs. affected) and for classification II (healthy or mild synovitis vs. moderate or severe synovitis).

| | Method A | Method B | Method C |
|---|---|---|---|
| Classification I | 0.65 | 0.57 | 0.65 |
| Classification II | 0.77 | 0.73 | 0.82 |

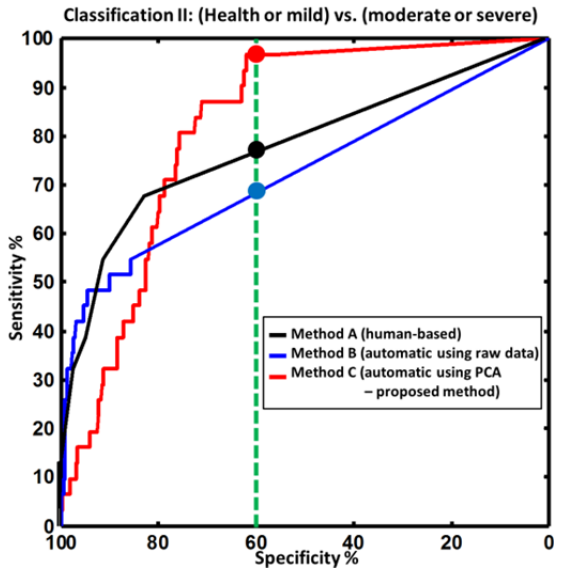


Figure 6: ROC curves for classification II: (healthy joint or mild synovitis) versus (moderate or severe synovitis), presented similar to the results presented for classification I in Figure 5. The green, dotted vertical line denotes a detection specificity of 60%. For this value, the proposed approach outperforms the human evaluation by achieving a sensitivity of more than 95% (human evaluation had a sensitivity of around 75%).

Figure 6 presents similar results for classification II. In this case, all methods perform better than the corresponding curves in classification I. This is justified as the signal difference between moderate synovitis and healthy or mild synovitis is generally larger than between healthy and mild synovitis. The proposed method C in this case has a markedly better performance than human reading. This improved performance can be seen examining the sensitivity values for a medium specificity value of 60% (as marked with filled circles on figure 6) or examining the AUC values, presented in Table 2.

## 8 DISCUSSION AND CONCLUSION

In this paper we presented automatic detection and characterization of synovitis in human hand joints using fluorescence images obtained in epi-illumination geometry post intravenous injection of ICG. The proposed method scores the principal components obtained from spatiotemporal analysis of the raw image sequences. The scores are then used to classify the synovitis in a binary fashion.

Two classification modes were examined: classification I (differentiating between healthy and affected joints) and classification II (differentiating between healthy or mild synovitis vs. moderate or severe synovitis). The automatic evaluation of fluorescence images was compared with the current methodology of human-based evaluation of images for both classification scenarios using ROC curves, as shown in Figures 5 and 6. The comparison of the proposed method with human-based reading was performed for a cohort consisting of 20 patients.

For classification I, as can be seen in Figure 5, all three methods A, B, and C have relatively low sensitivity. The reason is that in classification I we differentiate between healthy and affected joints. Around 22% (according to Table 2) of all joints have mild arthritis. However, mild joints exhibit only very low signal contrast relative to the healthy joints. This issue lowers the sensitivity of all methods. However, the proposed method has better sensitivity than the human detection for medium specificity levels. For classification II, however, the proposed method outperformed human detection in both sensitivity and AUC terms.

It should be noted that for both classification I and II, the methods A and B have higher sensitivity than the proposed method, for very high specificity values (> ~80%), as seen in Figures 5 and 6. However, these higher sensitivity values are

generally lower than 50%, which translate to a high count of missed positives for the respective threshold values.

The results generally show improved or comparable diagnostic performance achieved using the proposed, automatic method in comparison to the human-based evaluation. It is foreseeable that better and more intelligent classification methods making use of all signal properties (and not just the extracted segmentation metric *S*) could lead to definitively better performance than human reading. Such improved detection can not only lead to better detection but can also improve the therapy monitoring utility of optical imaging by reducing operator dependency. Such improved classification is being currently researched. Furthermore, semi-quantitative scoring of synovitis using optical images as well as further development of the proposed method in conjunction with larger cohorts are subjects of ongoing work.

## REFERENCES


Backhaus, M., Kamradt, T., Sandrock, D., Loreck, D., Fritz, J., Wolf, K. J., Raber, H., Hamm, B., Burmester, G. R. & Bollow, M. 1999. Arthritis Of The Finger Joints: A Comprehensive Approach Comparing Conventional Radiography, Scintigraphy, Ultrasound, And Contrast-Enhanced Magnetic Resonance Imaging. *Arthritis Rheum,* 42**,** 1232-45.

Chen, W. T., Mahmood, U., Weissleder, R. & Tung, C. H. 2005. Arthritis Imaging Using A Near-Infrared Fluorescence Folate-Targeted Probe. *Arthritis Research & Therapy,* 7**,** R310-R317.

Delle Sedie, A., Riente, L. & Bombardieri, S. 2008. Limits And Perspectives Of Ultrasound In The Diagnosis And Management Of Rheumatic Diseases. *Modern Rheumatology,* 18**,** 125-131.

Emery, P. & Quinn, M. A. 2003. Window Of Opportunity In Early Rheumatoid Arthritis: Possibility Of Altering The Disease Process With Early Intervention. *Clinical And Experimental Rheumatology,* 21**,** S154-S157.

Emery, P., Wakefield, R. J., O'connor, P. J., Conaghan, P. G., Mcgonagle, D., Hensor, E. M. A., Gibbon, W. W. & Brown, C. 2007. Finger Tendon Disease In Untreated Early Rheumatoid Arthritis: A Comparison Of Ultrasound And Magnetic Resonance Imaging. *Arthritis & Rheumatism-Arthritis Care & Research,* 57**,** 1158-1164.

Fawcett, T. 2006. An Introduction To Roc Analysis. *Pattern Recognition Letters,* 27**,** 861–874.

Fischer, T., Ebert, B., Voigt, J., Macdonald, R., Schneider, U., Thomas, A., Hamm, B. & Hermann, K. G. 2010. Detection Of Rheumatoid Arthritis Using Non-Specific Contrast Enhanced Fluorescence Imaging. *Acad Radiol,* 17**,** 375-81.

Gompels, L. L., Lim, N. H., Vincent, T. & Paleolog, E. M. 2010. In Vivo Optical Imaging In Arthritis--An Enlightening Future? *Rheumatology (Oxford),* 49**,** 1436-46.

Hielscher, A. H., Kim, H. K., Montejo, L. D., Blaschke, S., Netz, U. J., Zwaka, P. A., Illing, G., Muller, G. A. & Beuthan, J. 2011. Frequency-Domain Optical Tomographic Imaging Of Arthritic Finger Joints. *Ieee Trans Med Imaging,* 30**,** 1725-36.

Hielscher, A. H., Klose, A. D., Scheel, A. K., Moa-Anderson, B., Backhaus, M., Netz, U. & Beuthan, J. 2004. Sagittal Laser Optical Tomography For Imaging Of Rheumatoid Finger Joints. *Physics In Medicine And Biology,* 49**,** 1147-1163.

Huttenlocher, D. P., Klanderman, G. A. & Rucklidge, W. J. 1993. Comparing Images Using The Hausdorff Distance. *Ieee Transactions On Pattern Analysis And Machine Intelligence,* 15**,** 850-863.

Jolliffe, I. T. 2002. *Principal Component Analysis*, Springer.

Klose, A. D., Hielscher, A. H., Hanson, K. M. & Beuthan, J. 1999. Two- And Three-Dimensional Optical Tomography Of Finger Joints For Diagnostics Of Rheumatoid Arthritis. *Proceedings Of Spie,* 3566**,** 151-160.

Meier, R., Thuermel, K., Moog, P., Noel, P., Ahari, C., Sievert, M., Dorn, F., Waldt, S., Schaeffeler, C., Werner, S., Golovko, D., Haller, B., Ganter, C., Weckbach, S., Woertler, K. & Rummeny, E. J. 2012. Detection Of Arthritis In The Hands Of Patients With Rheumatological Disorders: Diagnostic Performance Of Optical Imaging In Comparison To Magnetic Resonance Imaging. *Arthritis & Rheumatism,* 64**,** 2489-98.

Meier, R., Thuermel, K., Noël, P. B., Moog, P., Sievert, M., Ahari, C., Nasirudin, R. A., Golovko, D., Haller, B., Ganter, C., Wildgruber, M., Schaeffeler, C., Waldt, S. & Rummeny, E. J. 2014. Synovitis In Patients With Early Inflammatory Arthritis Monitored With Quantitative Analysis Of Dynamic Contrast-Enhanced Optical Imaging And Mr Imaging. *Radiology,* 270**,** 176-185.

Michael Levandowsky & Winter, D. 1971. Distances Between Sets. *Nature,* 234**,** 34-35.

Mohajerani, P., Koch, M., Thürmel, K., Haller, B., Rummeny, E. J., Ntziachristos, V. & Meier, R. 2014. Fluorescence-Aided Tomographic Imaging Of Synovitis In The Human Finger. *Radiology*.

Mohajerani, P., Meier, R., Noël, P. B., Rummeny, E. J. & Ntziachristos, V. 2013. Spatiotemporal Analysis For Indocyanine Green-Aided Imaging Of Rheumatoid Arthritis In Hand Joints. *Journal Of Biomedical Optics,* 18**,** 097004-097004.

Ostergaard, M., Ejbjerg, B. & Szkudlarek, M. 2005. Imaging In Early Rheumatoid Arthritis: Roles Of Magnetic Resonance Imaging, Ultrasonography, Conventional Radiography And Computed Tomography. *Best Practice & Research In Clinical Rheumatology,* 19**,** 91-116.

Ostergaard, M., Peterfy, C., Conaghan, P., Mcqueen, F., Bird, P., Ejbjerg, B., Shnier, R., O'connor, P., Klarlund, M., Emery, P., Genant, H., Lassere, M. & Edmonds, J. 2003. Omeract Rheumatoid Arthritis Magnetic Resonance Imaging Studies. Core Set Of Mri Acquisitions, Joint Pathology Definitions, And The Omeract Ra-Mri Scoring System. *Journal Of Rheumatology,* 30**,** 1385-1386.

Thomas Dziekan, Carmen Weissbach, Jan Voigt, Bernd Ebert, Rainer Macdonald, Malte L. Bahner, Marianne Mahler, Michael Schirner, Michael Berliner, Birgitt Berliner, Jens Osel & Osel, I. 2011. Detection Of Rheumatoid Arthritis By Evaluation Of Normalized Variances Of Fluorescence Time Correlation Functions. *Journal Of Biomedical Optics* 16**,** 076015

Werner, S. G., Langer, H. E., Ohrndorf, S., Bahner, M., Schott, P., Schwenke, C., Schirner, M., Bastian, H., Lind-Albrecht, G., Kurtz, B., Burmester, G. R. & Backhaus, M. 2012. Inflammation Assessment In Patients With Arthritis Using A Novel In Vivo Fluorescence Optical Imaging Technology. *Annals Of The Rheumatic Diseases,* 71**,** 504-510.

Zou, K. H., O'malley, A. J. & Mauri, L. 2007. Receiver-Operating Characteristic Analysis For Evaluating Diagnostic Tests And Predictive Models. *Circulation,* 115**,** 654-7.